ASPERITY MODELS TO PREDICT SURFACE FAULT DISPLACEMENT CAUSED BY EARTHQUAKES: THE 2010 Mw 7.0 DARFIELD (NEW ZEALAND) EARTHQUAKE

L.A. DALGUER[1,4], H. WU[2], Y. MATSUMOTO[3], K. IRIKURA[4], T. TAKAHAMA[3] and M. TONAGI[3]

[1] Consultant, Switzerland

[2] Geo-Research Institute, Japan

[3] KOZO KEIKAKU ENGINIEERING Inc., Japan

[4] Aichi Institute of Technology, Japan

E-mail contact of main author: luis.dalguer@alumni.ethz.ch

Abstract. Asperity models for ground motion prediction is widely used in Japan. Here we expand the application of these asperity models to predict fault displacement caused by surface rupture. The 2010 Mw 7.0 Darfield (New Zealand) earthquake is used as a case study to model the fault displacement caused by this earthquake. Surface-rupturing was observed in several sites along the main fault reaching values of fault displacement larger than 5m. The main fault of this earthquake is strike-slip, almost vertical. Therefore, a simplified planar fault asperity model to capture the main features of the fault displacement is here developed. The fault dimensions are assumed to have a length of 60km and a width of 24km. First the fault is characterized by three asperities based on the kinematic asperity source model following the Irikura's Recipe (Irikura and Miyake, 2010) for strong ground motion prediction. Then, guided by this model, a dynamic fault rupture model is developed, in which asperities and background are characterized, respectively, by positive and zero stress drop. The first step to build the dynamic rupture model is assuming that the fault is buried. A trial and error procedure to estimate the stress drop on the asperities is followed, so that the average slip at each asperity be consistent with the ones from the kinematic model. At this stage, the dynamic model predicts strong ground motion consistent with those from the kinematic model. The preferred model predicts an earthquake of Mw 6.98 with average slip for each asperity of 2.7, 2.7, and 2m corresponding, respectively, to stress drops of 6.0MPa, 8.5MPa, and 7.0MPa. The second step is to include surface rupture by calibrating the weak shallow layer (WSL) (first 3km depth) with stress drop, strength excess (SE) and critical slip distance (Dc), so that the final fault displacement along the fault be consistent with the observed one. Within the framework of the asperity model, we found that negative stress drop is not necessary in the WSL, because this strongly inhibits surface rupturing. Our preferred model (from a total of 5 models that break the free surface) produces fault displacement distribution closer to the observed ones, but average slip at each asperity increases to 3.4m, 3.2 and 2.8m. This increase in average slip is due to the contribution of surface rupturing. The ground motion (velocity and displacement) from our preferred model is compared with observed records in the frequency band of 0.0 to 0.2Hz. Overall synthetics seismograms are consistent with observations. Ground motion differences between fault-surface rupturing and buried models are negligible, except at the very near-source. The differences originate only due to the WSL rupture that mainly affect the ground motion at the very near-source. Fault displacements are considered as potential hazards for nuclear facilities, long bridges and other structures founded across or near the fault. Empirical methods to predict fault displacement are few and not well constrained because of the sparseness of observed data. Therefore, the use of finite fault rupture models, as presented in this paper, provide valuable insights to evaluate fault displacement for future earthquakes.

Key Words: Dynamic rupture, fault displacement, asperity model, near-source ground motion.

1. INTRODUCTION

Kinematic finite fault rupture models characterized with asperity patches for strong ground motion prediction of scenario earthquakes is becoming current practice and widely used in Japan for earthquake disaster mitigation of urbanized cities and critical facilities (e.g. Kamae and Irikura, 1998; Irikura and Miyake, 2010). These asperity models have been also used to parameterize stress drop for fully physics based dynamic rupture models (e.g. Dalguer et al, 2004, 2008). The simplicity of these types of models that use independent constraints from empirical relationships and physical foundations make asperity models very attractive for practical application in seismic hazard studies. The kinematic asperity model currently used in practice in Japan for strong ground motion prediction is the so called Irikura's Recipe (Irikura and Miyake, 2010). This Recipe was designed to capture energy radiation from the seismogenic zone deeper than 2-3km, therefore it does not account for the radiation from the shallow layered (SL) zone and surface rupturing. The main future of the SL zone is that the radiation is dominated by long period ground motion. When the SL zone breaks the free-surface fault displacement and large permanent displacement arise, the latter sometimes named "fling" in the earthquake engineering community (Abrahamson, 2002; Burks and Baker, 2014; Kamai et al, 2014). Recent efforts to include these long period ground motion in the Irikura's Recipe is being developed by Irikura and Kurahashi (2018). However, fault displacement prediction (defined as the surface rupture offset or slip on the free-surface) is not included yet in the Recipe. Surface rupturing has been observed in some events such the 1999 Kocaeli (e.g. Akkar and Gülkan, 2002), 1999 Chi-Chi (e.g. Shin andTeng, 2001, Dalguer et al, 2001), 2002 Denali (e.g. Dreger et al, 2011), 2008 Wenchuan (e.g. Lu et al, 2010), 2011 Tohoku (e.g. Galvez et al, 2016) 2016 Kumamoto (Shirahama et al, 2016). Fault displacements are considered as potential hazards for nuclear facilities, long bridges and other structures founded across or near the fault. Empirical methods to predict fault displacement are few and not well constrained because of the sparseness of observed data. Therefore, prediction of fault displacement based on physics-based models is necessary because these models can provide more meaningful quantification and patterns of fault displacement. In the framework of asperity models, in the present paper we aim to expand the application of asperity models to predict fault displacement caused by surface rupture using dynamic rupture models. Unlike of kinematic models, dynamic models incorporate the physical processes involved in the fault rupture, taking into account conservation laws of continuum mechanics, constitutive behavior of rocks under interface frictional sliding, and state of stress in the crust. These idealization has proven to be a useful foundation for analyzing natural earthquakes (e.g. Andrews, 1976 ; Day, 1982, Olsen et al., 1997, Dalguer et al 2008, Galvez et al 2016).

The 2010 Mw 7.0 Darfield (New Zealand) earthquake is used as a case study for the asperity model to simulate the fault displacement caused by this earthquake. This event is one of the best-recorded earthquakes of this magnitude. Surface-rupturing was observed in several sites along the main fault, suggesting that rupture reached the surface. As shown in Figure 1 from the study reported by Quigley (2012), surface rupture has been observed at west, central and east segments with maximum values of 5.3m at the central segment. The rupture process and near-source ground motion seem also complex. 8 stations recorded peak accelerations larger than 0.5g, and some of them exceeded 1g (e.g., Fry and Benites, 2010). The earthquake was well captured with many local strong motion recordings (Figure 2). The fault geometry of this earthquake is rather complex composed with about 8 segments. The earthquake has initiated slowly in a branched fault, and then jumped to the main fault and propagates with high rupture speed in a geometrically complex fault with step-over toward the east and branched toward west.

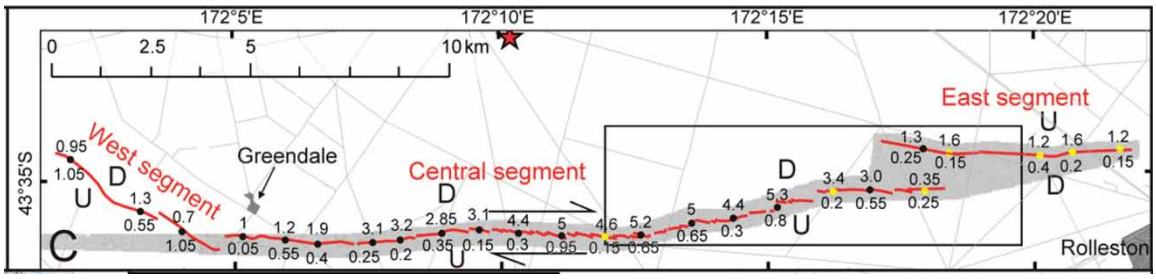

Figure 1. Detail fault trace map of surface rupture (red line). U and D are relative up and down sides. Numbers above the surface rupture line are measured horizontal fault offset, and below are vertical fault offset (after Quigley et al, 2012).

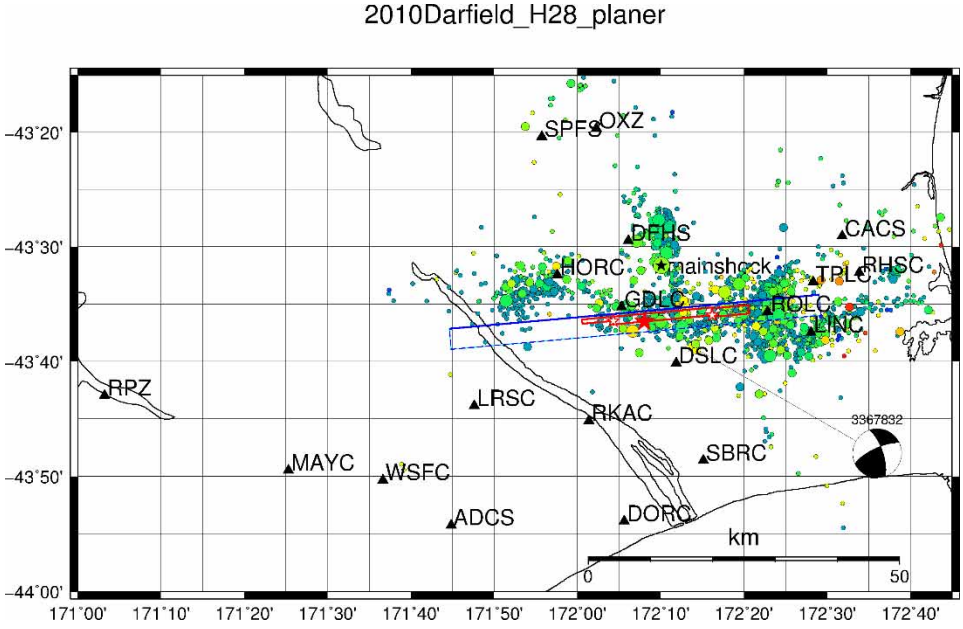

Figure 2. Location of near source stations, aftershock distribution and projection of a simplifies planar fault (blue line) with dip angle 82 degree for the dynamic rupture simulation.

In this paper we develop a simplified planar fault (Figures 2 and 3). Our main goal is to evaluate the surface rupture (fault displacement) and near-source ground motion. Since our model is based on the kinematic asperity model developed following Irikura's Recipe, the dynamic model is calibrated in two steps. The first step is to calibrate the dynamic asperity model in an embedded fault, so that the final slip of dynamic model be consistent with that from the kinematic model. In the second step the SL zone is included so that the fault displacement generated by the dynamic model be consistent with the observed one. Slip weakening friction in the form given by Andrews (1976) is used as constitutive model for dynamic rupture simulation.

2. Dynamic Rupture Model

First the fault is characterized by three asperities based on the kinematic asperity source model following the Irikura's Recipe (Irikura and Miyake, 2010) for strong ground motion prediction. Then, guided by this model, a dynamic fault rupture model is developed, in which asperities and background are characterized, respectively, by positive and zero stress drop. The first step to build the dynamic rupture model is assuming that the fault is buried. A trial and error procedure to estimate the stress drop on the asperities is followed, so that the average slip at

each asperity be consistent with the ones from the kinematic model. The second step is to include surface rupture by calibrating the weak SL zone (first 3km depth) with stress drop, strength excess (SE) and critical slip distance (Dc), so that the final fault displacement along the fault be consistent with the observed one.

The dynamic rupture models and near-source ground motion simulations have been developed using the Support Operator Rupture Dynamics code (SORD). The SORD code developed by Ely et al., (2008, 2009) uses a generalized Finite Difference (FD) scheme that can utilize structured hexahedral grids to mesh irregular geometry following a second-order accurate support operator scheme (e.g., Shashkov, 1996) with the capability to model general fault geometry and topography. SORD solves the three-dimensional visco-elastodynamic equations of motion; its scheme is explicit in time. The fault is represented by the split-node technique (Day et al, 2005; Dalguer and Day, 2006, 2007). The dynamic rupture occurs as dictated by the local stress conditions following a given constitutive law of friction. The code is parallelized, using Message Passing Interface (MPI), for multiprocessor execution, and is highly scalable, enabling large-scale earthquake simulations. The dynamic rupture model has been validated through the Southern California Earthquake Centre (SCEC) dynamic rupture code validation exercise, showing good agreement with semi-analytical boundary integral methods (Harris et al., 2009)

2.1. Fault model and velocity structure

The simplified dynamic rupture model is a strike slip planar fault with dip angle of 82 degree. The parameterization of the stress parameters is based on a kinematic asperity model developed using Irikura's Recipe. As shown in Figure 3 (left side), the fault dimensions are assumed to have a length of 60km and a width of 24km. The kinematic fault model is composed of three asperities named as ASP1, ASP2 and ASP3 with a respective average slip 2.5m, 2.5m, and 2m. The 1D velocity structure proposed by Guidotti et al.(2011) as illustrated in Figure 3 (right side) is used.

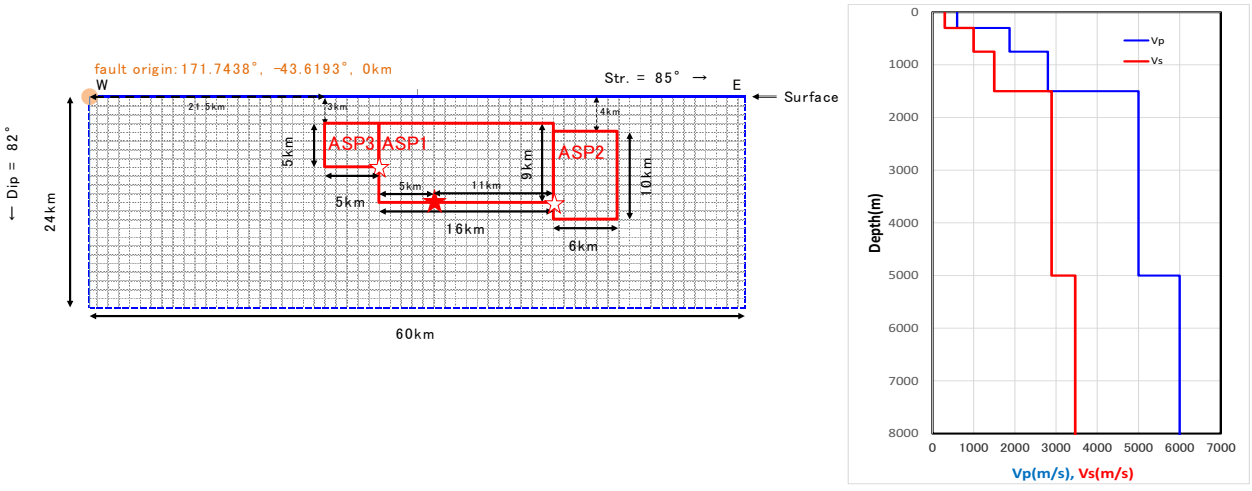

Figure 3. [left] Simplified asperity model in a planar fault developed using Irikura's Recipe. [right] 1D velocity structure (Guidotti et al.,2011) for the dynamic rupture simulation.

2.2.First step for dynamic parameterization

The first step for the dynamic rupture calculation is to find a model consistent with the kinematic asperity model in an embedded fault. The initial stress drop distribution is computed given the distribution of static slip from the kinematic model. For this purpose, we use the

approach from Andrews (1980) and expanded by Ripperger and Mai (2004). This simplified method relates stress drop and slip distribution in the wave number domain, in which stress drop is equal to the static stiffness matrix times the slip. Therefore, the calculation of stress drop for a given slip requires the 2D-Fourier Transform of the slip into the wave number domain. Then, require inverse transformation of the stress drop to back into the space domain (Ripperger and Mai, 2004). After calculating the initial stress drop distribution, a trial and error procedure is followed to estimate the stress drop at each asperity, so that the average slip at each asperity be consistent with the ones from kinematic model. 7 asperity models without surface rupture have been developed in this first step. The stress drop distribution, strength excess and critical slip distance for the asperity model 7 (preferred model) is shown in Figure 4 (left column). The background stress drop in the seismogenic zone is assumed to be zero, and a weak shallow layer (SL) zone of the first 2km depth is assumed to operate during rupture with enhanced energy absorption mechanism, as such it is parameterized with negative stress drop.

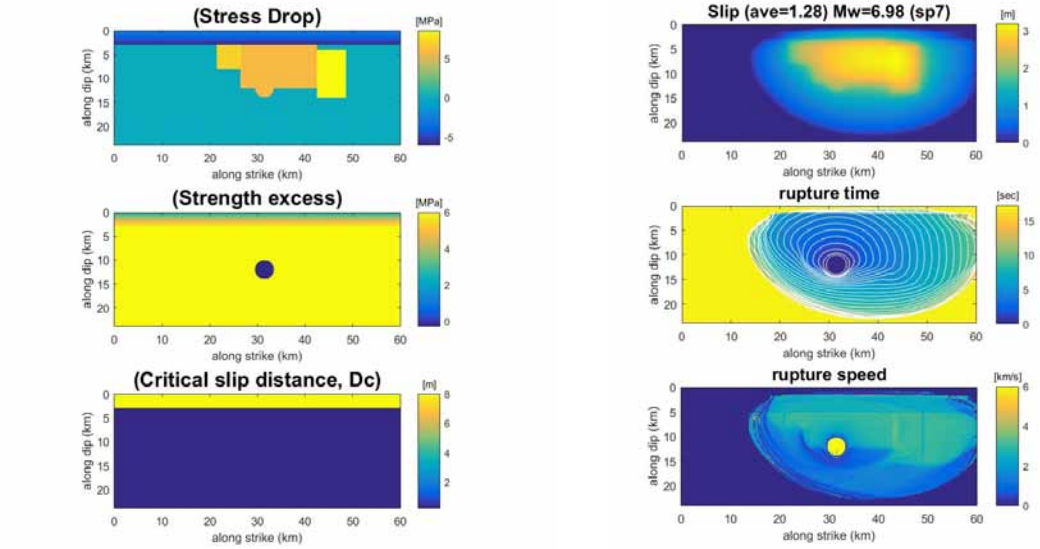

Figure 4. [left] Stress drop, strength excess and critical slip distance distribution for the dynamic rupture simulation of asperity model 7 without surface rupture consistent with the kinematic asperity model. [right] Dynamic rupture solution of asperity model 7, represented by final slip distribution (top), rupture time (middle) and rupture speed (bottom)

The asperity model 7 predicts an earthquake of Mw 6.98 with average slip for each asperity (ASP1, Asp2 and ASP3), respectively, 2.7, 2.7, and 2m, corresponding to stress drops of 6.0MPa, 8.5MPa, and 7.0MPa. Right column of Figure 4 shows the dynamic rupture solution of this model, represented by the final slip distribution, rupture time and rupture speed. Rupture time is about 12 seconds and rupture speed is sub-shear.

2.3.Second step of dynamic parameterization

In this second step, the SL zone parameterization is calibrated, while keeping the same parameterization of the seismogenic zone (model 7) developed in the first step (Figure 4), so that surface rupture be approximately consistent with observed fault displacement reported by Quigley (2012) as shown in Figure 1. For this purpose, 16 additional models have been developed. From them, 5 models break the free surface. We started varying the stress drop and strength excess at the SL zone for Dc values in the range of 0.5m to 8m. With this trial, we found that larger values of Dc > 3m and negative stress drop was not necessary in the SL, because they strongly inhibit surface rupturing. Figure 5 shows a profile of the dynamic parameterization (stress drop, strength excess, critical slip distance) along dip of a section crossing the center of the first asperity (ASP1 shown in Figure 3) for all the models that break

the free-surface (solid line) and some models (including model 7) without surface rupturing (dashed line). In this figure 5 (right side) is also presented the along strike average slip profile plotted with dip. This figure shows that models with surface rupturing enhance considerable the final slip distribution due to surface rupturing. All the surface rupturing models have nearly the same final slip at the sesmogenic zone. Notice that Model 20 (no surface rupture) has also the same final slip as the surface rupturing models at the seismogenic zone. This models did not break the free-surface because the presence of negative stress drop at the SL.

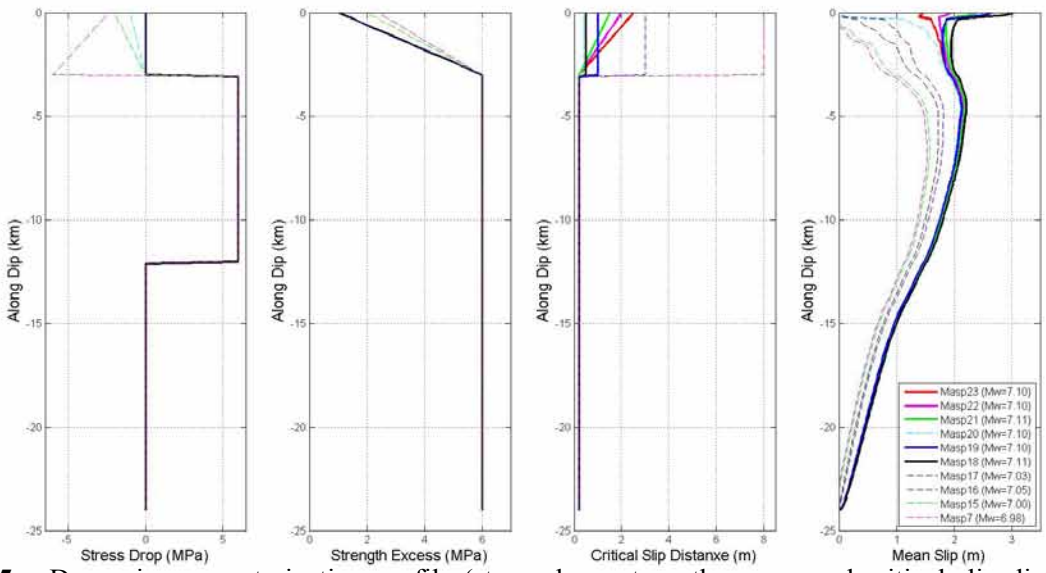

Figure 5. Dynamic parameterization profile (stress drop, strength excess and critical slip distance) along dip crossing the center of asperity 1 (ASP1 in Figure 3) from all models with surface rupturing (solid line) and some models without surface rupturing (dashed line) including Model 7 from Figure 4. Right side of this figures is shows the along strike average final slip profile of these models.

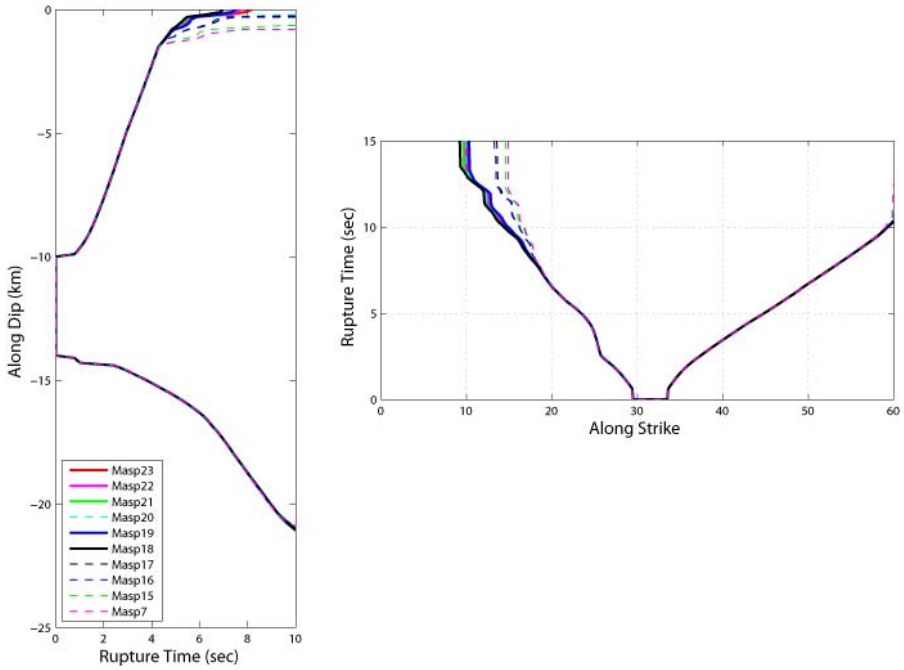

Figure 6. Rupture time along dip (left) and along strike (right) for sections respectively crossing the hypocenter. Solid lines are all models that break the free-surafce, and dashed line some models without surface rupturing, including model 7 from Figure 4.

The rupture propagation (rupture time and rupture speed) in the seismogenic zone is nearly the same for all the models (with and without surface rupturing). This is because the dynamic rupture parameterization at this zone is the same for all the models. This can be seen in Figure 6, in which rupture time along dip and along strike for sections respectively crossing the hypocenter are shown. Along dip, rupture time differ only at the shallow zone due to different parametrization at the SL zone. Along strike, the visible difference is seen at the west side (left side) due to rupture extension from models that break the free-surface.

3. Fault displacement

In order to evaluate which of the models with surface rupturing can be considered as best model consisting with observations, we compare the fault offset (fault displacement) distribution along strike with the measured fault offset (Figure 1) reported by Quigley et al (2012). We calculate the final offset from the horizontal and vertical component of fault offset for the west, central and east fault segment as defined by Quigley et al (2012). The location of the measured fault offset has been approximately adapted to our fault model. Figure 7 shows the synthetic fault displacement of all the models with surface rupturing compared with the measured fault offset. Notice that all the models, except model 23, extend the surface rupturing to wider areas compared to the observed ones. Though model 23 does not predict the maximum amplitude, in terms of distribution it is consistent with observations. However, it is important to mention that the observed fault offset (Figure 1) seems that occurs in three fault segments that are not spatially interconnected. This geometrical fault feature is different to our simplified dynamic models composed with only one planar fault segment. This simplification in our model is a limitation for better prediction of fault displacement.

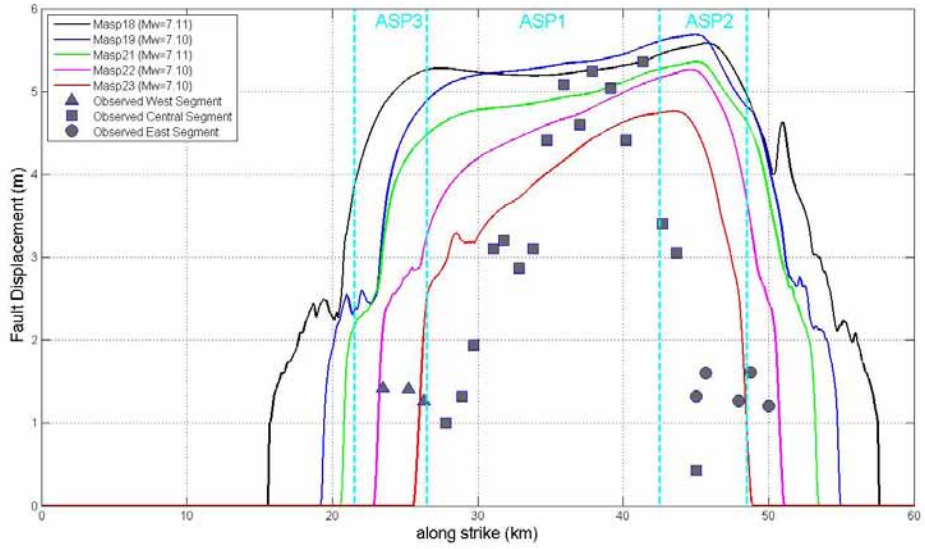

Figure 7. Comparison of synthetic fault displacement (solid lines) from all models that break the free-surface with observed fault offset reported by Quigley et al (2012). Model 23 is considered as the preferred model for being better consistent with the observed spatial distribution.

4. Dynamic rupture solution of preferred model

As mentioned above, our preferred model (model 23) produces fault displacement distribution closer to the observed ones (Figure 7). But compared to model 7, the average slip at the asperities increase to 3.4m, 3.2 and 2.8m, respectively for ASP1, ASP2 and ASP3. This increase in average slip is due to the contribution of surface rupturing, resulting an earthquake of Mw 7.1. This preferred model has dynamic parameterization at the SL (as shown in Figure 5) of

strength excess (SE) and critical slip distance (Dc) varying linearly from the seismogenic zone to the free surface, respectively from 6MPa to 1MPa for SE and from 0.2m to 2.5m for Dc. Stress drop is zero at the SL zone. Left side of Figure 8 shows the stress drop, strength excess and critical slip distribution on the fault for model 23. Right side of Figure 8 shows the dynamic solution of this preferred model represented by the final slip, rupture time and rupture speed distribution. Source parameterization and rupture propagation (rupture speed and rupture time) at the seismogenic zone are identical to the model 7 (Figure 4), as well as final slip pattern. The strong differences between these two models are at the SL zone.

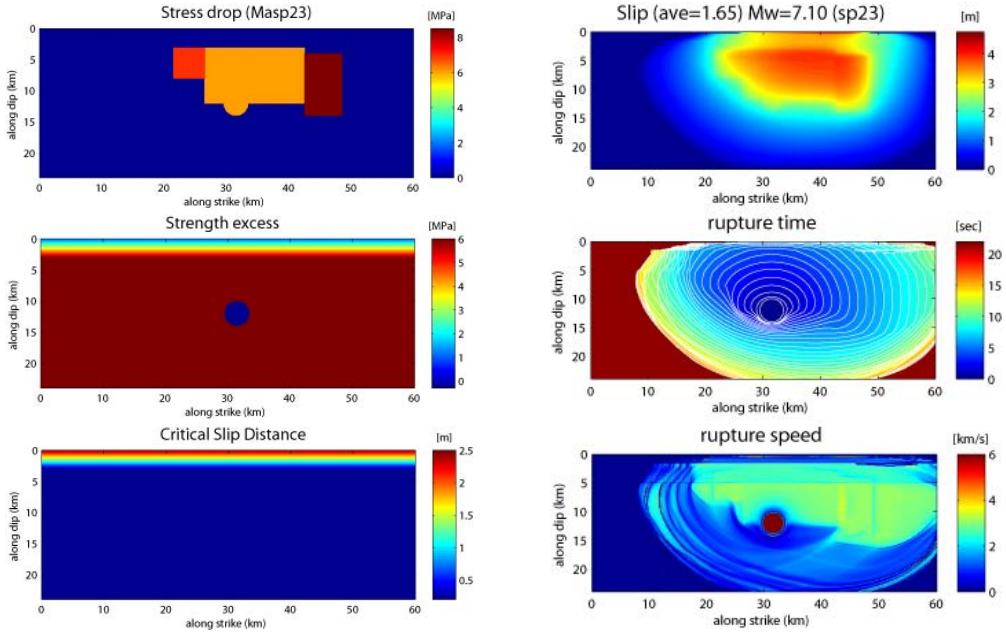

Figure 8. [left] Stress drop, strength excess and critical slip distance distribution for the dynamic rupture simulation of asperity model 23 with surface rupture consistent with observed fault offset [right] Dynamic rupture solution of asperity model 7, represented by final slip distribution (top), rupture time (middle) and rupture speed (bottom)

The slip velocity functions, filtered with a low pass filter with frequency cut of 0.5Hz, at different locations are plotted in Figure 9. They are plotted on the top of the final slip distribution. Notice the remarkable slip velocity pulses at surface rupture with amplitudes up to 4.0m/s, while inside the SL zone the slip velocity functions are smooth long period waveforms with lower amplitudes. These pulses at the free-surface generate large permanent displacements at the near-source pulse ground motion, sometimes named “fling”, resulted from surface-rupturing faulting. This suggest that the fling-pulses are maybe mainly caused by the abrupt surface rupturing rather than the asperities at the depth or rupture directivity effects. All the models that break the free-surface generate similar slip velocity function at the surface rupture, and at depth are nearly identical. The models with buried rupture also produce similar slip velocity function, but only at the seismogenic zone because of the same stress parameterization. Figure 10 shows these features when comparing slip velocity functions between the buried rupture (model 7) and the surface rupturing models 23 and 18. Though model 23 has been selected as our preferred model, because fault displacement in terms of extension along the fault is better consistent with observation, the model 18 is better consistent in term of maximum amplitude of fault displacement. Therefore, these two models, and the other surface rupturing models that are in between, can equally be considered good models in terms of ground motion, as will be discussed in the next section

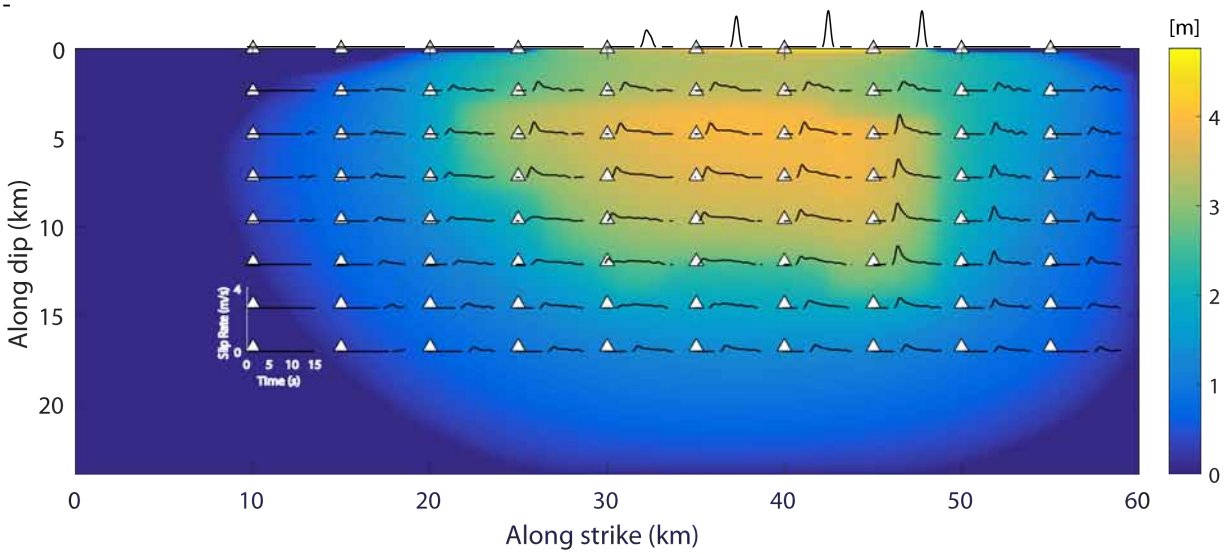

Figure 9. Slip velocity functions distributed at some points on the fault from the model 23. Background correspond to the final slip distribution from the same model.

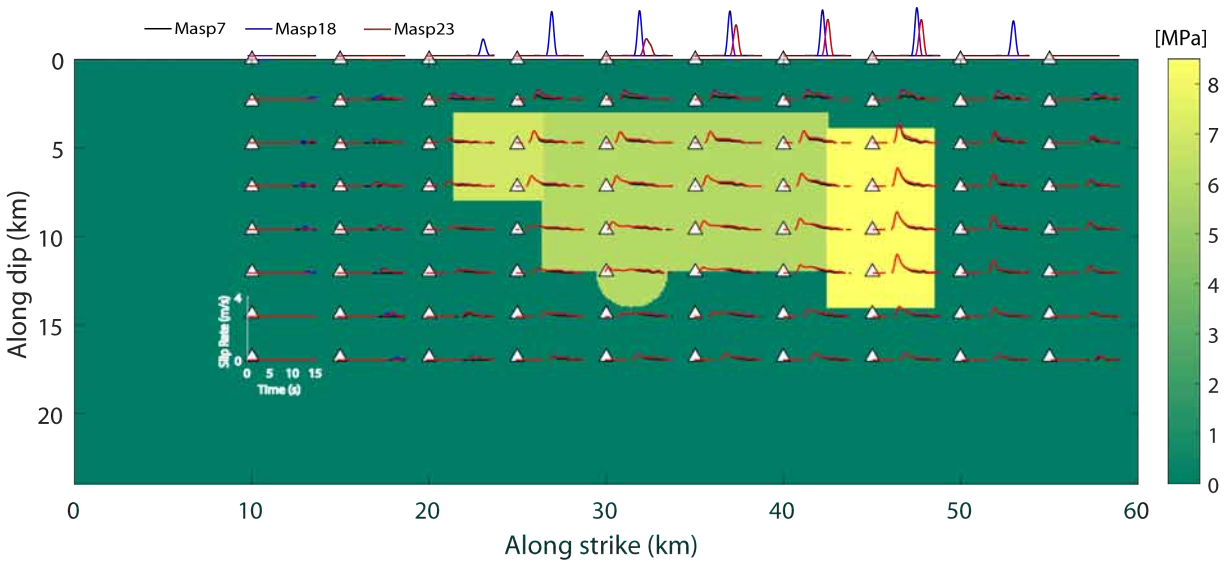

Figure 10. Slip velocity functions distributed at some points on the fault from models 7, 18 and 23. Background correspond to the stress drop distribution of surface rupturing models (18 and 23)

5. Ground Motion: surface rupturing vs buried fault

We have also simulated ground motion at the stations shown in Figure 2. Considering that the source rupture parameterization at the seismogenic zone is for surface rupturing and buried models, as shown in Figure 5 and 6, ground motion differences between these models arises only due to the surface rupturing. Therefore, these differences are seen at the very near-source. Here we show comparison with observation for the EW component that best fitting has been obtained at the very near source. The closest station to the fault is station GDLC (see figure 2). Figure 11 shows velocity and displacement for surface rupturing and buried models compared with observed one. The surface rupturing model is consistent with observation, in particular for the first velocity pulse and displacement offset. The difference with the buried rupture is

evident. Buried rupture model at this station does not predict observations. Now in Figure 12 we compare with station relatively far from the fault (station SPFS, see Figure 2). Though the comparison with observation for the two models is not optimum, remarkable is that the differences between the two models (surface rupture and buried) is minor. In summary, ground motion at far distance is similar for buried and surface rupturing and at very near stations differences are evident, in particular for the displacement. Comparison is done in the frequency band of 0.0 to 0.2Hz.

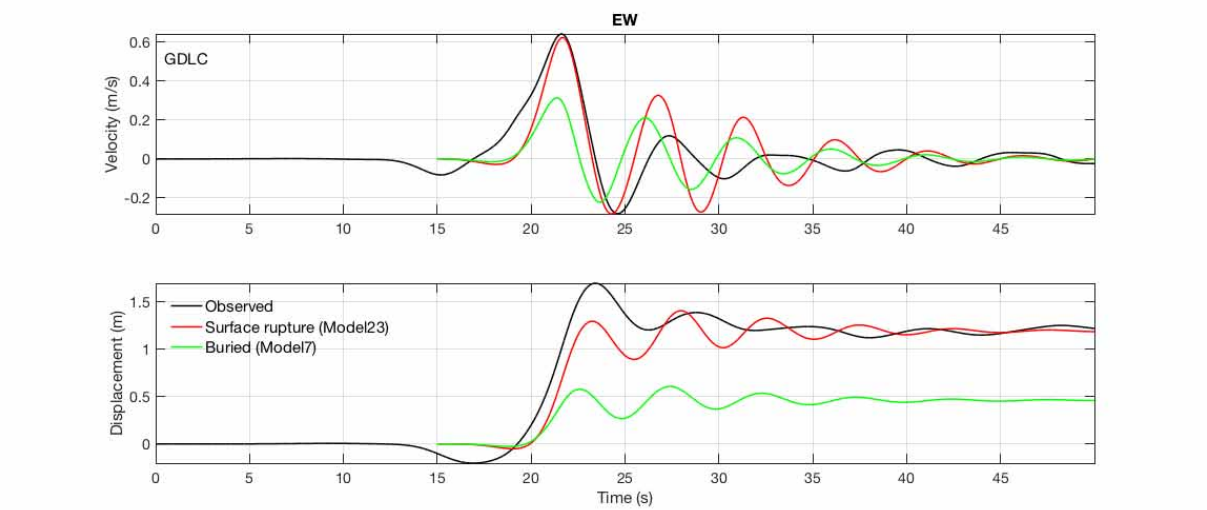

Figure 11. EW components of velocity and displacement ground motion compared with observation and between buried model 7 and surface rupturing models 23 for Station GDLC (very near to the fault).

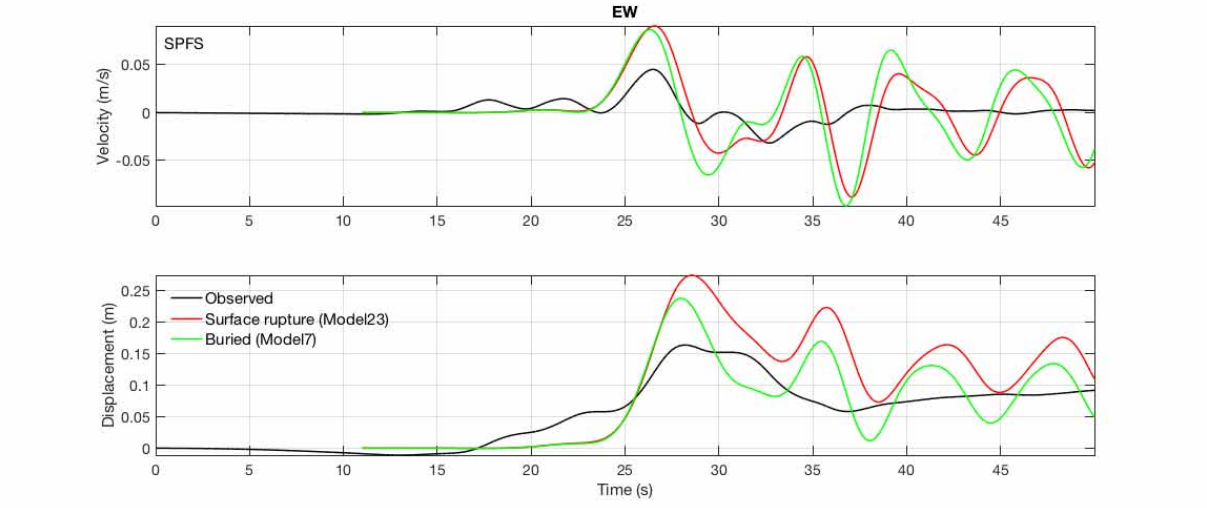

Figure 12. EW components of velocity and displacement ground motion compared with observation and between buried model 7 and surface rupturing models 23 for Station SPFS (far distance to the fault).

6. Conclusions

We have developed dynamic asperity models for the 2010 Mw 7.0 Darfield (New Zealand) earthquake to evaluate fault displacement and near source ground motion. The dynamic rupture parameterization uses as constraint the kinematic asperity model developed following Irikura's Recipe. The first step of the dynamic parameterization uses a buried fault model to fit the kinematic slip model. The reason to use buried model is because Irikura's Recipe does not account for the ground motion generated by the shallow layer zone and fault displacement. Then in the second step, the shallow layer zone with surface rupturing is included to model fault displacement. At this second step, the dynamic parameterization of the seismogenic zone developed in step 1 remains the same. Then calibration of the shallow layer zone uses as constraint the observed fault displacement. We found that negative stress drop is not necessary in the shallow zone, because this strongly inhibits surface rupturing. The ground motion differences between the buried models (step1) and surface rupturing models (step 2) is minor as far distances, however at the very near-source is evident due to the surface rupturing effects. Our study suggests that the inclusion of the shallow zone effects and surface rupture are necessary for ground motion prediction very near to the source. Fault displacements are considered as potential hazards for nuclear facilities, long bridges and other structures founded across or near the fault. Empirical methods to predict fault displacement are few and not well constrained because of the sparseness of observed data. Therefore, the use of finite fault rupture models, as presented in this paper, provide valuable insights to evaluate fault displacement for future earthquakes.

Acknowledgement: This research was part of the 2015-2016 research project 'Development of evaluating method for fault displacement' by the Secretariat of Nuclear Regulation Authority (NRA), Japan.

REFERENCES

Abrahamson NA (2002), Velocity pulses in near-fault ground motions, *in Proceedings of the UC Berkeley—CUREE Symposium in Honor of Ray Clough and Joseph Penzien*: Berkeley, California, UC Berkeley, Consortium of Universities for Research in Earthquake Engineering, 9–11 May 2002, 40–41.

Akkar S, Gülkan P (2002), A Critical Examination of Near-Field Accelerograms from the Sea of Marmara Region Earthquakes, *Bull. Seism. Soc. Am.* **92**, 1, pp. 428–447.

Andrews, D.J (1976). Rupture velocity of plane-strain shear cracks, *J. Geophys. Res.*, 81, 5679-5687.

Andrews, D. J. (1980), A stochastic fault model: 1. Static case, *J. Geophys. Res.*,85, 3867–3877.

Burks LS, Baker JW (2014): Fling in near-fault ground motions and its effect on structural collapse capacity, *in Tenth U.S. National Conference on Earthquake Engineering, Frontiers of Earthquake Engineering*, Anchorage, Alaska, 21–25 July 2014.

Dalguer, L. A. and Day, S. M. (2006), Comparison of Fault Representation Methods in Finite Difference Simulations of Dynamic Rupture. *Bull. Seismol. Soc. Am,* 96, 1764 - 1778.

Dalguer, L. A. and Day, S. M. (2007), Staggered-Grid Split-Nodes Method for Spontaneous Rupture Simulation. *J. Geophys. Res.,* 112, B02302, doi:10.1029/2006JB004467

Dalguer, L.A., H. Miyake, S.M. Day and K. Irikura (2008), Surface Rupturing and Buried Dynamic Rupture Models Calibrated with Statistical Observations of Past Earthquakes. *Bull. Seismol. Soc. Am.* 98, 1147-1161, doi: 10.1785/0120070134.

Dalguer LA, Irikura K, Riera J, Chiu HC (2001) : The Importance of the Dynamic Source Effects on Strong Ground Motion During the 1999 Chi-Chi (Taiwan) Earthquake: Brief Interpretation of the Damage Distribution on Buildings. *Bull. Seismol. Soc. Am*., 95, 1112-1127.

Dalguer, L. A., H. Miyake, and K. Irikura (2004). Characterization of dynamic asperity source models for simulating strong ground motion, *Proceedings of the 13th World Conference on Earthquake Engineering (13WCEE),* Vancouver, B.C., Canada, August 1-6, 2004, Paper No. 3286.

Day, S. M. (1982). Three-dimensional simulation of spontaneous rupture: the effect of nonuniform prestress, *Bull. Seismol. Soc. Am.,* 72, 1881-1902.

Day, S. M., L.A. Dalguer, N. Lapusta, and Y. Liu (2005). Comparison of finite difference and boundary integral solutions to three-dimensional spontaneous rupture, *J. Geophys. Res.,* 110, B12307, doi:10.1029/2005JB003813.

Dreger D, Hurtado G, Chopra A, Larsen S (2011): Near-Field Across-Fault Seismic Ground Motions, *Bull. Seism. Soc. Am.*, Vol. 101, No. 1, pp. 202–221, February 2011, doi: 10.1785/0120090271

Ely, G. P., S. M. Day and J.-B. Minster (2008). A support-°©-operator method for viscoelastic wave modelling in 3-°©-D heterogeneous media, *Geophysical Journal International,* 172(1) 331-344.

Ely, G., S. M. Day and J-B. Minster (2009). A support-operator method for 3D rupture dynamics, *Geophysical Journal International,* 177 1140-1150, DOI: 10.1111/j.1365 246X.2009.04117.x.

Galvez P, Dalguer LA, Ampuero JP, Giardini D (2016): Rupture reactivation during the 2011 Mw 9.0 Tohoku earthquake: Dynamic rupture and ground motion simulations, *Bull. Seismol. Soc. Am.,* Vol. 106, No. 3, pp. –, June 2016, doi: 10.1785/0120150153.

Guidotti, R., Stupazzini, M., Smerzini, C., Paolucci, R. and Ramieri, P., 2011, Numerical Study on the Role of Basin Geometry and Kinematic Seismic Source in 3D Ground Motion Simulation of the 22 February 2011 MW 6.2 Christchurch Earthquake, *Seismological Research Letters,* 82, 767-782.

Harris, R. A., M. Barall, R. Archuleta, E. M. Dunham, B. Aagaard, J. P. Ampuero, H. Bhat, V. Cruz-Atienza, L. Dalguer, P. Dawson, S. Day, B. Duan, G. Ely, Y. Kaneko, Y. Kase, N. Lapusta, Y. Liu, S. Ma, D. Oglesby, K. Olsen, A. Pitarka, S. Song, and E. Templeton (2009), The SCEC/USGS dynamic earthquake-rupture code verification exercise, *Seismological Research Letters,* 80(1), 119-126, doi:10.1785/gssrl.80.1.119.

Irikura and Kurahashi (2018), Extension of strong-motion-prediction recipe for near-source long-period ground motion: Validation of ground motion for the 2016 Mw 7.0 Kumamoto earthquake in Japan. *Proceeding of the BestPSHANI 2018 workshop Best Practices in Physics-based Fault Rupture Models for Seismic Hazard Assessment of Nuclear Installations: issues and challenges towards full Seismic Risk Analysis,* Cadarache-Château, France, 14-16 May 2011.

Irikura, K., and H. Miyake (2011). Recipe for predicting strong ground motion from crustal earthquake scenarios, *Pure Appl. Geophys.*, 168, 85-104, doi:10.1007/s00024-010-0150-9.

Kamae, K. and K. Irikura (1998), Source model of the 1995 Hyogo-ken Nanbu earthquake and simulation of near-source ground motion, *Bull. Seism. Soc. Am.,*, 88, 2, 400-412,1998.

Kamai R, Abrahamson N, Graves R (2014) : Adding Fling Effects to Processed Ground-Motion Time Histories. *Bull. Seism. Soc. Am.,* Vol. 104, No. 4, pp. 1914–1929, August 2014, doi: 10.1785/0120130272.

Lu M, Jun Li X, Wen An X, Zhao J.X (2010): A Preliminary Study on the Near-Source Strong-Motion Characteristics of the Great 2008 Wenchuan Earthquake in China, *Bull. Seism. Soc. Am.*, Vol. 100, No. 5B, pp. 2491–2507, November 2010, doi: 10.1785/0120090132.

Olsen, K. B., R. Madariaga, and R. Archuleta (1997). Three Dimensional Dynamic Simulation of the 1992 Landers Earthquake, *Science.* 278, 834-838.

Pitarka, A., L.A. Dalguer, S.M. Day, P. Somerville, and K. Dan (2009). Numerical study of ground motion differences between buried and surface-rupturing earthquakes, *Bull. Seism. Soc. Am.* , Vol. 99, No. 3, pp. 1521–1537, June 2009, doi: 10.1785/0120080193

Quigley, M; R. Van Dissen, N. Litchfield, P. Villamor, B. Duffy, D. Barrell, K. Furlong, T. Stahl, E. Bilderback and D. Noble (2012). Surface rupture during the 2010 Mw 7.1 Darfi eld (Canterbury) earthquake: Implications for fault rupture dynamics and seismic-hazard analysis, *GEOLOGY*, vol. 40; no. 1; p. 55–58; doi:10.1130/G32528.1

Ripperger, J., and P.M. Mai (2004). Fast computation of static stress changes on 2D faults from final slip distributions, *Geophys. Res. Lett.*, Vol. 31, No. 18, L18610 10.1029/2004GL020594.

Shashkov, M. (1996). Conservative Finite-Difference Methods on general grids, *CRC Press,* Boca Raton, FL.

Shin TC, Teng TL (2001): An overview of the 1999 Chi-Chi, Taiwan, earthquake, *Bull. Seism. Soc. Am.* **91,** 895–913.

Shirahama, Y., M. Yoshimi, Y. Awata, T. Maruyama, T. Azuma, Y. Miyashita, H. Mori, K. Imanishi, N. Takeda, T. Ochi, M. Otsubo, D. Asahina and A. Miyakawa (2016), Characteristics of the surface ruptures associated with the 2016 Kumamoto earthquake sequence, central Kyushu, Japan, *Earth, Planets and Space* 68:191 DOI 10.1186/s40623-016-0559-1.